Functionalized Thermo-responsive Microgels for High Performance Forward Osmosis Desalination

Yusak Hartanto, Seonho Yun, Bo Jin*, Sheng Dai*

School of Chemical Engineering, The University of Adelaide, SA 5005, Australia

*Corresponding authors:

E-mail: s.dai@adelaide.edu.au; bo.jin@adelaide.edu.au

Abstract

Stimuli-responsive hydrogels were recently proposed for energy-saving forward osmosis (FO) process. However, their low water flux and dewatering ability for reuse make them unsuitable for desalination process. In this work, the co-polymer microgels of N-isopropylacrylamide and acrylic acid with different mixing ratios were synthesized using surfactant-free emulsion polymerization to produce submicron-size hydrogels with high surface area and fast swelling-deswelling response. The microgels were employed as draw agents in a laboratory scale FO desalination system to treat synthetic brackish water. The microgel-based FO process displayed a high water flux up to 23.8 LMH and high water recovery ability up to 72.4%. In addition, we explored a new approach to measure water flux via the on-line conductivity measurement of feed solution. This on-line conductivity analysis approach appeared to be an accurate and efficient method for evaluating microgel-based FO desalination performance. Our experimental data revealed that the stimuli-responsive microgel was an efficient draw agent for FO desalination.

Keywords: microgels; forward osmosis; desalination; water flux; dewatering ability; N-isopropylacrylamide; on-line conductivity; thermo-responsive

1. Introduction

Water scarcity is one of the top global challenges that currently affects over one-third of world population in water-stressed countries and this situation is worsen due to increasing population, water pollution, industrialization, and climate change (McCutcheon et al., 2006; Elimelech and Phillip, 2011). Over 96 % of water resources worldwide are in the ocean, which have high salinity and cannot be directly used without desalination process (Smalley, 2005). To date, reverse osmosis (RO) process via a polymeric membrane is the most widely used technology for seawater desalination. However, the high energy and capital costs together with the low water permeability and fouling resistance associated with RO membrane have been an on-going challenge for its industrial applications. There is a pressing need for the development of a cost-effective desalination process.

In the recent years, forward osmosis (FO) membrane process has gained a lot of attention due to its potential as low energy membrane separation process. The FO desalination is a two-stage desalination process where the water is drawn from a saline solution as a result of osmotic gradient and then the water can be recovered from draw solute by means of membrane separation, distillation, external magnetic field, extraction, precipitation and combination of these separation processes (Luo et al., 2014). Inorganic salts, such as $MgCl_2$, $MgSO_4$, NaCl, KCl, $KHCO_3$, $Ca(NO_3)_2$, NH_4HCO_3 have been employed as the draw solutes for FO processes (Achilli et al., 2010). Although these inorganic reagents have excellent capability to create significant osmotic pressure gradient, pressure-driven membrane processes such as nanofiltration and reverse osmosis are still required to recover water from these salts (Zhao et al., 2012). That leads to an increase in the energy consumption for the overall FO process. Furthermore, reverse salt flux and internal concentration polarization are presented when these salts are employed as draw solutes, which subsequently reduce the

performance of separation process. Scientists found that the use of ammonium bicarbonate (NH_4HCO_3) as the draw agents could lead to a low energy FO process, as water can be recovered via low temperature distillation process using low grade heat (McCutcheon et al., 2006; McGinnis and Elimelech, 2007). The draw solute can decompose into ammonia and carbon dioxide upon heating and leave water phase. Unfortunately, the purity of water resulted from such process was not able to meet standard drinking water regulation due to very high ammonium bicarbonate leaked to the water product (Ge et al., 2013).

Subsequent research proposed that poly(ethyleneglycol)diacid-coated superparamagnetic nanoparticles could be used as draw solutes and the adsorbed water can be recovered using external magnetic field to produce fresh water (Ge et al., 2010). However, water flux performance was far below the water flux generated by inorganic salts. Furthermore, these magnetic nanoparticles formed aggregates during the recovery stage which decreased their effectiveness to be reused (Ling and Chung, 2011; Ling et al, 2011). Other materials have also been explored for FO processes, including the sodium salt of polyacrylic acid (Ge et al., 2012), 2-methylimidazole-based organic compounds (Swee Kuan et al., 2010), switchable polarity solvent (Stone et al., 2013), hydroacid complexes (Ge and Chung, 2013), Na^+ functionalized carbon quantum dots (Guo et al., 2014) and N,N',N"-triacylated tris(2-aminoethyl)amine (acyl-TAEA) derivatives (Noh et al., 2012). Although these materials displayed reasonable water flux, their low water recovery ability is a drawback for their applications in industrial desalination processes.

Stimuli-responsive hydrogels are three dimensional polymer networks that swell and deswell in respond to the applied stimuli, such as temperature, pH, external magnetic field, ionic strength, and light. Due to their ability to reversibly swell and deswell, they have been recently introduced as a new class of draw agent for FO desalination. In the early study, the

hydrogel was synthesized using N-isopropylacrylamide and hydrophilic monomers of sodium acrylate or acrylamide (Li et al., 2011). The water contained in the hydrogels was recovered by heating the hydrogels and applying pressure. Unfortunately, the water flux of this hydrogels (0.30-0.96 LMH) with salt rejection of 95.4% was relatively lower than other types of synthetic draw agents. In order to improve the performance of hydrogels-based FO process, composite hydrogels were recently prepared by incorporating inorganic nanoparticles such as carbon particles, magnetic nanoparticles and reduced graphene oxide (rGO) (Razmjou et al., 2013a; Zeng et al., 2013). These composite hydrogels showed an enhanced water flux and the water recovery ability. However, the recovered water from hydrogels was mostly in the form of water vapour. Additional condensation unit is then needed to recover water in the form of liquid and will increase the overall costs of FO process.

Currently, the high energy costs for water recovery is still an issue for FO desalination technologies (Altaee et al., 2014). This leads to higher operational cost of FO desalination compared to RO process due to inappropriate selection of water recovery process and materials employed as draw solutes (McGovern and Lienhard V, 2014). Other major limitations are incomplete separation of draw agents and lower water flux compared to the RO process (Cai et al., 2013). In this study, we applied N-isopropylacrylamide (NIPAM) and acrylic acid (AA) as co-monomers to synthesize functional co-polymer microgels P(NIPAM-AA) as the draw agents for FO process. The microgels with different ratios of AA and NIPAM were prepared using surfactant-free emulsion polymerization (SFEP) approach to eliminate the contamination of small surfactants. Moreover, a laboratory FO system was established to evaluate the desalination performance of the P(NIPAM-AA) microgel-based FO process. Our results show that the employed P(NIPAM-AA) microgels can significantly improve water flux and water recovery ability of the FO desalination process. For the first

time, we use microgels in FO desalination process. The microgels are also functionalized with acrylic acid rather than sodium acrylate to improve the water flux. Besides, we explored and employed new on-line conductivity monitoring method to analyse water flux of the FO system.

2. Materials and methods

2.1. Materials

N-isopropylacrylamide (NIPAM, > 98%), purchased from Tokyo Chemical Industry, was purified by recrystallization in n-hexane and dried at room temperature. N-N'-methylenebisacrylamide (MBA, >98%), acrylic acid (AA, >99.5%) and ammonium persulfate (APS) were purchased from Sigma-Aldrich. Sodium chloride was purchased from VWR. Cellulose triacetate forward osmosis (CTA-FO) membranes were purchased from Hydration Technologies Inc. (HTI, USA).

2.2. Synthesis of co-polymer microgels

The P(NIPAM-AA) microgels were synthesized using surfactant-free semi-batch emulsion polymerization. In a typical experiment, 0.5 g of NIPAM and AA at different mass ratios and 0.005 g of MBA were dissolved in 47 mL of Millipore water. The solution was transferred to a 250 mL three-necked flask fitted with a condenser, a mechanical stirrer and gas inlet/outlet. The semi-batch feeding solution was prepared by dissolving 2.5 g of NIPAM and AA at different mass ratios, 0.025 g of MBA and 0.025 g of APS in 30 mL of Millipore water.

After degassing both batch and semi-batch feeding solutions for one hour, the batch solution was heated to 75 °C under nitrogen atmosphere. 3.0 mL of APS solution (0.005 g) was injected to initiate the polymerization. Semi-batch feeding solution was injected slowly at a rate of 6.25 mL/hour using a syringe pump after the batch solution turned into cloudy. The

polymerization was carried out overnight under continuous stirring. After cooling, the microgels were purified using membrane dialysis (MWCO 12–14 kDa) against Millipore (or DI) water for three days. During three days purification, the water was changed every two hours. The purification was confirmed by comparing the conductivity of dialysis water and the conductivity of Milipore (or DI) water. The purified microgels were dried at 70 ºC and grounded into fine powders.

2.3. Conductometric and potentiometric titration

The amount of acrylic acid in the microgels was quantified using conductometric and potentiometric titration. Typically, the pH of a 100 mL P(NIPAM-AA) microgel dispersion (~ 1 mg/mL) was adjusted to pH 3 using hydrochloric acid. The solution was then back titrated using 0.1 M NaOH. After each addition of NaOH, the solution conductivity and pH were measured using a pre-calibrated Aqua-CP/A pH and conductivity meter.

2.4. Dynamic light scattering

The hydrodynamic diameters (d_h) of the synthesized P(NIPAM-AA) microgels were measured by dynamic light scattering (DLS) at different temperatures using a Zetasizer (Malvern, Nano-ZS). The DLS data were collected on an autocorrelator and the CONTIN software package was used to analyse the intensity autocorrelation functions. The swelling ratio (SR) of microgels can be calculated using the following equation:

$$SR = \left(\frac{d_{h,25}}{d_{h,40}}\right)^3 \quad (1)$$

where SR is the swelling ratio of the microgels, $d_{h,}25$ (nm) is the hydrodynamic diameter of the microgels at 25 ºC and $d_{h,40}$ (nm) is the hydrodynamic diameter of the microgels at 40 ºC.

2.5. Water flux evaluation

100 mg of grounded microgel powders were placed in our customized membrane setup equipped with on-line conductivity monitoring system as shown in Figure 1. The photo of this laboratory on-line conductivity monitoring system for FO process can be found in Figure S1 (Supporting Information). Calibrated conductivity probe (with probe cell constant, k = 1.0) was immersed in the feed solution of 2000 ppm NaCl to continuously monitor the conductivity against time for five hours. The conductivity data can be converted into the concentration of sodium chloride after fitting with the following equation:

$$\lambda = 1.7821 C_t \quad (2)$$

where λ is the conductivity of feed solution (μS/cm) and C_t is the feed concentration at time t (ppm).

The water flux was calculated using the conductivity data based on the mass balance equation which is described by the following equations:

$$V_t = \frac{C_i V_i}{C_t} \quad (3)$$

$$J_W = \frac{V_i - V_t}{A_{eff}\,\Delta t} \quad (4)$$

where V_t (mL) is the volume of feed at time t, V_i (mL) is the initial volume of feed, C_i (ppm) is the initial feed concentration, C_t (ppm) is the feed concentration at time t, J_w (LMH) is the water flux, A_{eff} (m^2) is the effective membrane surface area and Δt (h) is the time interval where the volume of the feed solution changes.

2.6. Water recovery

After five hours, the swelled microgels were transferred to centrifuge tubes and weighed. The swelled microgels were then centrifuged at 40 ºC and 12,000 rpm for 10 minutes to separate

adsorbed water from polymer microgels. The recovered water was determined using gravimetric analysis. The water recovered from microgel deswelling was calculated using the following equations:

$$\mathbf{C_P} = \frac{\mathbf{W_P}}{\mathbf{W_P + W_W}} \quad (5)$$

$$W_{WG} = W_H(1\text{-}C_P) \quad (6)$$

$$R = \frac{W_R}{W_{WG}} \text{x } 100\% \quad (7)$$

where C_P (g microgels/g H_2O) is the concentration of microgels in the centrifuge tube, W_P (g) is the weight of dry microgel powders, W_W (g) is the weight of water adsorbed by the microgels determined from water adsorption from water flux measurement, W_{WG} (g) is the weight of water in the microgels, W_H (g) is the weight of microgels in the centrifuge tube, W_R (g) is the weight of adsorbed water recovered from the tube and R (%) is the percentage of water recovered from the deswelled microgels .

2.7. Microgels recycling in three cycles

The swelled microgels after the 1st cycle were dried in oven until constant weights. The dried microgels were grounded into fine powders and placed in our FO system for the 2nd cycle measurement, where the conductivity readings of sodium chloride solution against time were recorded to calculate water flux. Similar approach was repeated for the 3rd cycle measurement.

3. Results and Discussion

3.1. Synthesis and characterization of the microgels

Semi-solid forward osmosis draw agent like stimuli-responsive hydrogels requires fast water absorption and releasing capability in order to produce high water flux and water recovery

rate. Unfortunately, hydrogels synthesized by bulk polymerization approach has slower water absorption and releasing rate compared to small hydrogels (microgels) synthesized using emulsion polymerization approach. This is due to the formation of dense skin layer in bulk hydrogels which retards water diffusion in and out of hydrogels (Hoare, 2012). For this reason, emulsion polymerization is chosen to overcome this problem to produce faster water absorption and releasing rate.

The conventional approach to synthesize microgels is emulsion polymerization where surfactants, such as sodium dodecyl sulphate (SDS), are added to the mixture of monomers, crosslinker and initiator to stabilize the formed microgels. The obtained microgels can be purified by dialysis against deionized water to remove surfactants and unreacted monomers. However, complete removal of all surfactant might not be possible. These unremoved surfactants could affect physio-chemical characteristics and performance of the microgels, depending upon their final applications (Pelton and Hoare, 2011). For example, the water adsorption capability of the microgels could be reduced in the presence of charged surfactants. For this reason, surfactant-free emulsion polymerization (SFEP) synthesis route was chosen in this study. Different from traditional emulsion polymerization, SFEP always produces monodisperse microgels. In addition, the synthesis was conducted in a semi-batch mode rather than a batch mode to produce high solids content of microgel suspension which is an effective technique for mass production of microgels to meet the industrial scale quantity of draw agent for microgels-based FO desalination. The yields of the microgels vary in a range of 70-90%, indicating most of feed monomers have been polymerized.

The amount of AA incorporated into the microgels can be calculated from pH and conductivity titration curves as shown in Figure S2 (Supporting Information). The calculated amount of AA incorporated into the microgels is above 75% of the feed for all microgels, indicating high conversions of AA during copolymerization. The high incorporation of AA is

crucial when doing copolymerization as some co-monomers are not readily incorporated due to their different reactivity ratios with other monomers (Sheikholeslami et al., 2012). Furthermore, dynamic light scattering was performed at different temperatures to determine the volume phase transition temperature (VPTT) of the microgels. This characterization method serves two main purposes, determination of individual microgel particle size and volume phase transition temperature (VPTT). Size larger than FO membrane pore size is needed to prevent leakage of microgels to the feed solution and hence minimizing draw agent replenishment. The volume phase transition temperature (VPTT) of microgels can be useful preliminary information on energy requirement of dewatering process of microgels. Microgels with higher VPTTs require more energy in the form of heat to raise their temperature and to recover the absorbed water. Dynamic light scattering was performed at different temperatures to determine the volume phase transition temperature (VPTT) of the microgels. The profiles of hydrodynamic diameter *vs.* temperature are shown in Figure 2a. Table 1 shows that the hydrodynamic particle sizes of the microgels at 25 ºC vary in a range of 200-300 nm. Below the transition temperatures, the microgels show a swelled state where polymers are fully hydrated. As temperature increases to phase transition temperatures, the microgels shrink significantly due to the dehydration of PNIPAM segments (Shen et al., 2014). As a result, the microgels can release up to 70% of water absorbed into bulk solution. Shen et al. (2012) observed that the VPTTs of these microgels did not change significantly as the AA mass varied between 0 wt% and 50 wt%. This result agrees well with the obtained VPTTs from our P(NIPAM-AA) microgels with AA varied from 0 to 70 wt% (Table 1).

While the AA content in this study does not affect the VPTTs of the microgels, the swelling ratios do vary with the AA contents in the microgels. The swelling ratios of the microgels with different AA contents at 40 ºC are shown in Figure 2b. As the AA content increases in a range of 0 – 70%, the swelling ratio decreases from 15.9 to 2.3. The microgels with a low AA

content (5% or 8%) display higher swelling ratio than those with a high content of AA (50% or 70%). That is due to the fact that PNIPAM moieties dominate the hydrophobic interaction in NIPAM-rich microgels. The high AA content microgels shrink slightly due to the strong electrostatic repulsion among these deprotonated carboxylic groups, preventing polymer network to collapse.

3.2. New method for water flux evaluation via conductivity measurement

The commonly used technique to quantify water flux is to measure the mass increase of hydrogels through gravimetric method, where the mass of swelled hydrogels is weighed at certain time intervals (Li et al., 2011; Razmjou et al., 2013a; Cai et al., 2013; Razmjou et al., 2013b; Razmjou et al., 2013c). However, this approach could lead to large systematic errors when the powder quantity is small. We found that the water flux data fluctuate during the measurement period, as presented in Figure S3 (Supporting Information). In this study, we developed a new approach to analyse water flux for batch microgel-based FO process. Due to the difference in the osmotic pressures of feed solution and microgels at both sides of FO membrane, water is transferred to microgels, resulting in changing the feed concentration with time (Wang et al., 2014). These concentration changes can be monitored using a conductivity meter. Our data revealed that conductivity measurement provides much more accurate results of water flux for laboratory based evaluation than the commonly used gravimetric method. Importantly, the conductivity analysis can provide efficient on-line measurements to determine desalination performance of FO process. The conductivity calibration curve in Figure 3 shows a linear relationship between sodium chloride concentration and solution conductivities, which was established using statistic regression method. Based on the calibration curve, the concentration of sodium chloride can be calculated from conductivity measurement based on Eq. 2. The variation in NaCl concentration can be further used to calculate the amount of water drawn by microgels using

Eq. 3. Then, the water flux can be estimated from Eq. 4 by dividing the water adsorption rate with effective membrane area.

Before each conductivity measurement, the FO membrane was allowed to soak in 2000 ppm NaCl solution overnight to reach an equilibrium condition (Li et al., 2011). The equilibrium condition is needed to saturate the FO membrane with sodium chloride and to minimize the diffusion of sodium chloride through the membrane. Furthermore, the transport of water molecules is faster than the transfer of sodium chloride through cellulose acetate membrane (Lonsdale et al., 1965). Hence, the assumption of no sodium chloride leakage during the water flux evaluation is valid. In addition, the conductivity probe was conditioned for 30 minutes in 2000 ppm NaCl solution prior to conductivity measurement to ensure that the conductivity changes are not affected due to external factors, such as temperature, possible NaCl adsorption on the membrane and equilibrium readings in conductivity meter. In order to validate the reproducibility of our new method of using conductivity measurement to calculate water flux, all experiments were conducted three times for each microgel. Figure 4 presents these calculated water flux results, indicating that a good repeatability of conductivity method for all microgels. Water flux for each sample follows a similar profile where high fluxes are observed during the first 5 to 10 minutes, resulting in a rapid change in conductivity. After 60 minutes, water flux declines rapidly and reaches equilibrium. In contrast, high water fluxes for bulk P(NIPAM) and bulk co-polymer of NIPAM and sodium acrylate hydrogels, P(NIPAM-SA), were observed during the first two hours and reached equilibrium after 7 hours (Li et al., 2011). The flux for P(NIPAM) hydrogels after 60 minutes was 0.30 LMH, while a water flux of 0.55 LMH was given by P(NIPAM-SA) hydrogels with 50 wt% of SA. Another study conducted by the same group, using the P(NIPAM-SA) hydrogel with 50 wt% of SA as a model draw agent, showed that the dimensions of the hydrogel affect water flux magnitudes. They reported that small hydrogel had a higher water

flux than the large one due to greater membrane contact area. The water fluxes for the hydrogels with sizes of 2-25 μm and 500-1000 μm were approximately 1.3 LMH and 0.8 LMH, respectively, in the first hour (Razmjou et al., 2013b). On the other hand, the water flux of our P(NIPAM) and P(NIPAM-AA) microgels with the same monomers were approximately 2 LMH and 4 LMH, respectively. The higher fluxes observed from our study can be the result of the large surface area of the microgels produced from surfactant-free emulsion polymerization. The large surface area of the microgels is beneficial for enhancing interfacial contact between microgels and FO membrane, and therefore results in a shorter time needed to reach the equilibrium condition compared to bulk hydrogels reported by Li et al. (2011). Table 2 summarises key results from this and previous studies on hydrogel-based FO process.

3.3. Effect of acrylic acid on water flux

In practice, thermo-responsive microgels are rarely polymerised from a single monomer. Co-monomers are usually employed to synthesize microgels with objectives to provide certain functionalities, such as dual-response microgels (temperature and pH), growing inorganic nanoparticles inside the microgels (Zhang et al., 2004), and enhanced swelling-deswelling ratios. Our results show that the AA contents in P(NIPAM-AA) can significantly influence the hydrophilic and hydrophobic properties of the microgels. Below the pKa of AA (~ 4.75), the AA moieties are hydrophobic after their protonation. As the pH is above the pKa of AA, the carboxylic groups become deprotonated and thus make the microgels be hydrophilic. The hydrophilic characteristic of the microgels at moderate pH will facilitate water adsorption.

Figure 4-f shows that the P(NIPAM-AA) microgels perform an improved water flux compared to the P(NIPAM) microgels. For example, the addition of 5% acrylic acid resulted in a significantly higher water flux of 21 LMH than the initial water flux of 8.9 LMH for the

303 microgels without AA incorporation. The flux increases slightly to 23.8 LMH when
304 microgels are synthesized with 8% AA. It is interesting to note the addition of excess AA
305 from 50% to 70% appears to have limited impact on the water flux of the co-polymer
306 microgels measured after five hours. The water flux after five hours absorption period for
307 P(NIPAM) microgels is 1.01 LMH, while P(NIPAM-AA) microgels with 5% and 8% AA
308 show a flux of 1.31 LMH and 1.62 LMH, respectively. A further increase in AA moieties to
309 50% and 70% results in slight improvement of water flux from 1.49 LMH to 2.05 LMH,
310 respectively. In summary, AA does not have important effect on the water flux when its
311 content is beyond 8% in the microgels.

312 The water fluxes of our microgels are higher than the hydrogels reported in previous study
313 (Li et al., 2011). The major reason might come from the structure-property relationship of
314 materials synthesized. In this work, we used emulsion polymerization method to synthesize
315 submicron-size gels as the building block for temperature responsive hydrogels compared to
316 those prepared by bulk polymerization in previous studies. This approach allows us to
317 produce submicron-size gels which have large surface area and fast response. As a result, the
318 water fluxes are improved significantly for microgels.

319 **3.4. Effect of acrylic acid on dewatering performance of the microgels**

320 As the temperature is above the VPTT, the PNIPAM moieties become hydrophobic, resulting
321 in shrinking the microgels, and consequently releasing the adsorbed water. However, AA
322 moieties do not change their chemical properties since the carboxylic groups only response to
323 pH variation. When the swelled microgels are heated to 40 ^{o}C, the co-polymer microgels with
324 up to 8% AA undergo a phase separation while the microgels incorporated with 50% or more
325 AA do not show obvious phase separation. As the AA content increases, the hydrophilicity of
326 the microgels increases because of the increment of carboxylic groups in microgels. This

means that microgels with a higher AA content can keep more water than the PNIPAM homopolymer microgels. As a result, an increase in AA has adverse effect on the recovery of adsorbed water as increasing temperature over their VPTTs.

Figure 5 shows that the dewatering ability of the microgels decreases as AA contents increase. Homopolymer PNIPAM microgels demonstrate the highest water recovery (72%), while the co-polymer P(NIPAM-AA) microgels with 5% and 8% AA have 55% and 52% water recovery. It is interesting to note that when the AA content in the microgels is high, such as 50% and 70%, almost no water can be recovered from the microgels at the temperature beyond the VPTT. However, when trace amount of hydrochloric acid is added to adjust the pH to about 5, a temperature of 40 ^{o}C can lead to a phase separation of the microgels with 50%wt of AA. The pH change using hydrochloric acid facilitates the protonation of carboxylate and relevant dewatering performance of microgels. The amount of water recovered from our microgel-based FO process is over 50% for PNIPAM-AA microgels which is higher than the water recovery from previous studies where only over 17% of absorbed water recovered (Li et al., 2011).

Increasing AA moieties has an opposite effect on water flux and water recovery in our microgel-based FO system. A high AA content of the microgels leads to an enhanced water flux, while reducing the water recovery. To determine the best microgels which show a balanced performance in water flux and water recovery, the water flux and water recovery are multiplied to give the overall water production rate from microgel-based FO process. Figure 6 presents the overall water production rates of FO process using the co-polymer P(NIPAM-AA) microgels. We note that overall FO performance is the function of the AA contents in microgels, and the microgel with 8% AA gives the best overall water production rate.

3.5. Recyclability of thermo-responsive microgels in forward osmosis

FO process relies on the reversible abilities of water adsorption and releasing of the draw agent. In order to examine the recycling ability of our thermo-responsive microgels for the reuse in the FO desalination, recycling experiments were carried out three times to assess the performance of water flux and water recovery. Homopolymer and co-polymer microgels with 8% AA are compared in this study in terms of their recovery recyclability. Figure 7 shows that both thermo-responsive homopolymer and co-polymer microgels demonstrate promising water flux and water recovery performance in the three recycling FO processes. Generally, the initial water flux remains constant throughout the subsequent cycles and the equilibrium swelling time remains the same as the first cycle except for the copolymer microgels with 8% AA where a slight decrease of water flux from 23.8 LMH to 20.6 LMH.

4. Conclusion

A series of co-polymer P(NIPAM-AA) microgels was prepared by surfactant-free emulsion polymerization. Their desalination performance in terms of water flux and dewatering ability were evaluated in a laboratory forward osmosis system. We for the first time developed an on-line conductivity method to evaluate water flux of microgel-based FO process. This method was confirmed as an accurate and efficient approach to assess the FO performance. The systematic results showed that the application of microgels can lead to a cost-effective FO desalination process. Co-polymer P(NIPAM-AA) microgels show comparably higher water flux and water recovery ability than those prepared by bulk polymerization, while a shorter equilibrium time for water adsorption is required. Thermo-responsive microgels also show promising recyclability of water absorption and water recovery.

Acknowledgement

The authors would like to thank the financial support from the Australian Research Council (DP110102877). YH would like to appreciate the support of Adelaide Graduate Research Scholarships (AGRS).

References

Achilli, A., Cath, T.Y. and Childress, A.E., 2010. Selection of inorganic-based draw solutions for forward osmosis applications. Journal of Membrane Science 364(1–2), 233-241.

Altaee, A., Zaragoza, G. and van Tonningen, H.R., 2014. Comparison between Forward Osmosis-Reverse Osmosis and Reverse Osmosis processes for seawater desalination. Desalination 336, 50-57.

Cai, Y., Shen, W., Loo, S.L., Krantz, W.B., Wang, R., Fane, A.G. and Hu, X., 2013. Towards temperature driven forward osmosis desalination using Semi-IPN hydrogels as reversible draw agents. Water Research 47(11), 3773-3781.

Elimelech, M. and Phillip, W.A., 2011. The Future of Seawater Desalination: Energy, Technology, and the Environment. Science 333(6043), 712-717.

Ge, Q., Su, J., Amy, G.L. and Chung, T.S., 2012. Exploration of polyelectrolytes as draw solutes in forward osmosis processes. Water Research 46(4), 1318-1326.

Ge, Q., Su, J., Chung, T.S. and Amy, G., 2010. Hydrophilic Superparamagnetic Nanoparticles: Synthesis, Characterization, and Performance in Forward Osmosis Processes. Industrial & Engineering Chemistry Research 50(1), 382-388.

Ge, Q.C. and Chung, T.S. (2013) Hydroacid complexes: a new class of draw solutes to promote forward osmosis (FO) processes. Chemical Communications 49(76), 8471-8473.

Ge, Q.C., Ling, M.M. and Chung, T.S. (2013) Draw solutions for forward osmosis processes: Developments, challenges, and prospects for the future. Journal of Membrane Science 442, 225-237.

398 Guo, C.X., Zhao, D., Zhao, Q., Wang, P. and Lu, X., 2014. Na(+)-functionalized carbon
399 quantum dots: a new draw solute in forward osmosis for seawater desalination. Chemical
400 Communications 50(55), 7318-7321.

401 Hoare, T. (2012) Hydrogel Micro and Nanoparticles, pp. 281-315, Wiley-VCH Verlag GmbH
402 & Co. KGaA.

403 Li, D., Zhang, X., Yao, J., Simon, G.P. and Wang, H., 2011. Stimuli-responsive polymer
404 hydrogels as a new class of draw agent for forward osmosis desalination. Chemical
405 Communications 47(6), 1710-1712.

406 Ling, M.M. and Chung, T.S., 2011. Desalination process using super hydrophilic
407 nanoparticles via forward osmosis integrated with ultrafiltration regeneration.
408 Desalination 278(1–3), 194-202.

409 Ling, M.M., Chung, T.S. and Lu, X.M., 2011. Facile synthesis of thermosensitive magnetic
410 nanoparticles as "smart" draw solutes in forward osmosis. Chemical Communications
411 47(38), 10788-10790.

412 Lonsdale, H.K., Merten, U. and Riley, R.L. (1965) Transport properties of cellulose acetate
413 osmotic membranes. Journal of Applied Polymer Science 9(4), 1341-1362.

414 Luo, H., Wang, Q., Zhang, T.C., Tao, T., Zhou, A., Chen, L. and Bie, X. (2014) A review on
415 the recovery methods of draw solutes in forward osmosis. Journal of Water Process
416 Engineering 4, 212-223.

417 McCutcheon, J.R., McGinnis, R.L. and Elimelech, M., 2006. Desalination by ammonia–
418 carbon dioxide forward osmosis: Influence of draw and feed solution concentrations on
419 process performance. Journal of Membrane Science 278(1–2), 114-123.

420 McGinnis, R.L. and Elimelech, M., 2007. Energy requirements of ammonia-carbon dioxide
421 forward osmosis desalination. Desalination 207(1-3), 370-382.

McGovern, R.K. and Lienhard V, J.H. (2014) On the potential of forward osmosis to energetically outperform reverse osmosis desalination. Journal of Membrane Science 469,245-250.

Noh, M., Mok, Y., Lee, S., Kim, H., Lee, S.H., Jin, G. W., Seo, J.H., Koo, H., Park, T.H. and Lee, Y., 2012. Novel lower critical solution temperature phase transition materials effectively control osmosis by mild temperature changes. Chemical Communications 48(32), 3845-3847.

Pelton, R. and Hoare, T., 2011. Microgel Suspensions, pp. 1-32, Wiley-VCH Verlag GmbH & Co. KGaA.

Razmjou, A., Barati, M.R., Simon, G.P., Suzuki, K. and Wang, H., 2013a, Fast Deswelling of Nanocomposite Polymer Hydrogels via Magnetic Field-Induced Heating for Emerging FO Desalination. Environmental Science & Technology 47(12), 6297-6305.

Razmjou, A., Liu, Q., Simon, G.P. and Wang, H., 2013c. Bifunctional Polymer Hydrogel Layers As Forward Osmosis Draw Agents for Continuous Production of Fresh Water Using Solar Energy. Environmental Science & Technology 47(22), 13160-13166.

Razmjou, A., Simon, G.P. and Wang, H., 2013b. Effect of particle size on the performance of forward osmosis desalination by stimuli-responsive polymer hydrogels as a draw agent. Chemical Engineering Journal 215–216, 913-920.

Sheikholeslami, P., Ewaschuk, C., Ahmed, S., Greenlay, B. and Hoare, T. (2012) Semi-batch control over functional group distributions in thermoresponsive microgels. Colloid and Polymer Science 290(12), 1181-1192.

Shen, Z., Bi, J., Shi, B., Nguyen, D., Xian, C.J., Zhang, H. and Dai, S., 2012. Exploring thermal reversible hydrogels for stem cell expansion in three-dimensions. Soft Matter 8(27), 7250-7257.

446 Shen, Z., Mellati, A., Bi, J., Zhang, H. and Dai, S., 2014. A thermally responsive cationic
447 nanogel-based platform for three-dimensional cell culture and recovery. RSC Advances
448 4(55), 29146-29156.
449 Smalley, R.E., 2005. Future global energy prosperity: The terawatt challenge. MRS Bulletin
450 30(6), 412-417.
451 Stone, M.L., Rae, C., Stewart, F.F. and Wilson, A.D., 2013. Switchable polarity solvents as
452 draw solutes for forward osmosis. Desalination 312, 124-129.
453 Swee Kuan, Y., Mehnas, F.N.H., Minglue, S., Kai Yu, W. and Tai-Shung, C., 2010. Study of
454 draw solutes using 2-methylimidazole-based compounds in forward osmosis. Journal of
455 Membrane Science 364(1-2), 242-252.
456 Wang, H., Wei, J. and Simon, G.P., 2014. Response to Osmotic Pressure versus Swelling
457 Pressure: Comment on “Bifunctional Polymer Hydrogel Layers As Forward Osmosis
458 Draw Agents for Continuous Production of Fresh Water Using Solar Energy”.
459 Environmental Science & Technology 48(7), 4214-4215.
460 Zeng, Y., Qiu, L., Wang, K., Yao, J., Li, D., Simon, G.P., Wang, R. and Wang, H., 2013.
461 Significantly enhanced water flux in forward osmosis desalination with polymer-
462 graphene composite hydrogels as a draw agent. RSC Advances 3(3), 887-894.
463 Zhang, J., Xu, S. and Kumacheva, E., 2004. Polymer Microgels: Reactors for
464 Semiconductor, Metal, and Magnetic Nanoparticles. Journal of the American Chemical
465 Society 126(25), 7908-7914.
466 Zhao, S., Zou, L. and Mulcahy, D., 2012. Brackish water desalination by a hybrid forward
467 osmosis–nanofiltration system using divalent draw solute. Desalination 284, 175-181.

Table 1 Synthesis and characterization of P(NIPAM-AA) microgels

Nomenclature	Monomer Content in Feed (g)		MBA	APS	AA content (mmol g^{-1} polymer)		Yield	d_h*	VPTT**
	NIPAM	AA	(g)	(g)	Observed	Theoretical	(%)	(nm)	(°C)
MCG-NP100-AA0	4.00	-	0.04	0.04	0	0	88	306	34
MCG-NP95-AA5	3.80	0.20	0.04	0.04	0.56	0.74	72	211	33
MCG-NP92-AA8	3.68	0.32	0.04	0.04	0.82	1.10	97	306	34
MCG-NP50-AA50	2.00	2.00	0.04	0.04	5.71	6.79	84	200	32
MCG-NP30-AA70	1.20	2.80	0.04	0.04	9.23	9.71	69	255	32

* Hydrodynamic diameters of microgels measured at 25 °C in water

**Determined from the tangent line of the inflexion point of hydrodynamic diameter *vs.* temperature curves

Table 2 Summary of the water flux and swelling equilibrium time of bulk hydrogels and microgels

Draw agents	Composition (wt%)			Synthesis Method	Particle size (μm)	Initial Water Flux (LMH)	Water Recovery (%)	Equilibrium Swelling Time (minutes)	References
	NIPAM	SA	AA						
Homo polymer Hydrogels	100	0	0	Bulk Polymerization	50-150	0.30	75	420	(Li et al., 2011)
Co-polymer Hydrogels	50	50	0			0.55	17		
Co-polymer Hydrogels	50	50	0	Bulk Polymerization	500-1000	0.8	-	600	(Razmjou et al., 2013b)
					2-25	1.3			
Microgels	100	0	0	Surfactant-free Emulsion Polymerization	0.306	2	72	60	This study
	50	0	50		0.200	4	-		

Figure

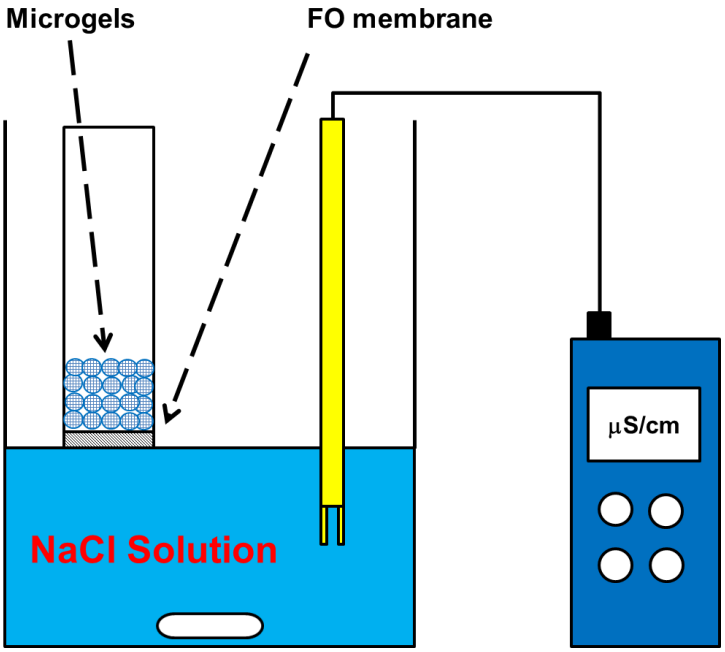

Figure 1. Forward osmosis setup using a conductivity probe to monitor water flux.

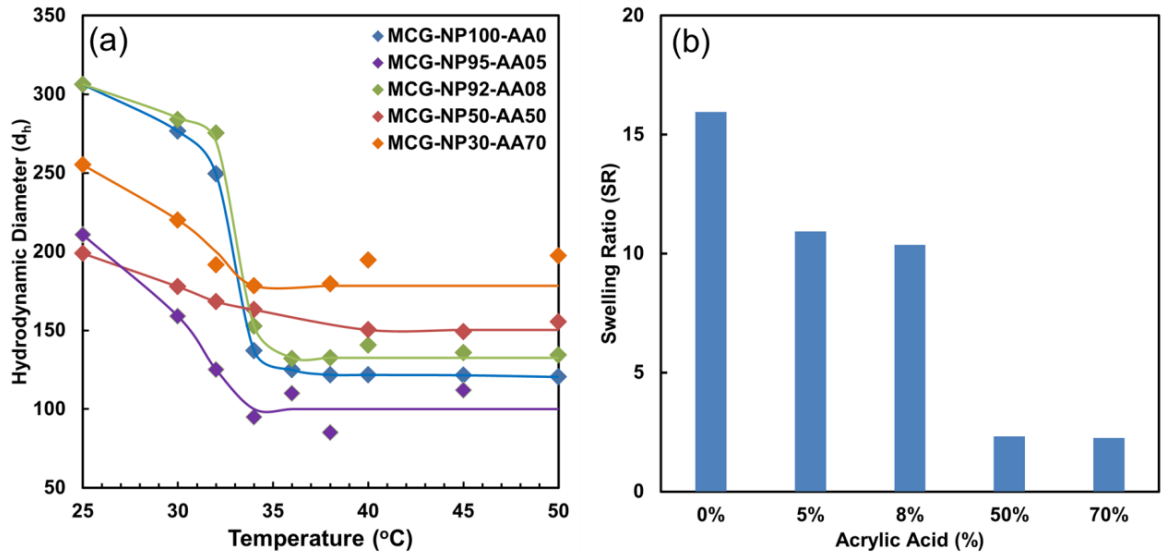

Figure 2. (a) Volume phase transition temperatures (VPTT) of P(NIPAM)-AA microgels with different of acrylic acid contents; and (b) Swelling ratios of various P(NIPAM-AA) microgels at 40 °C.

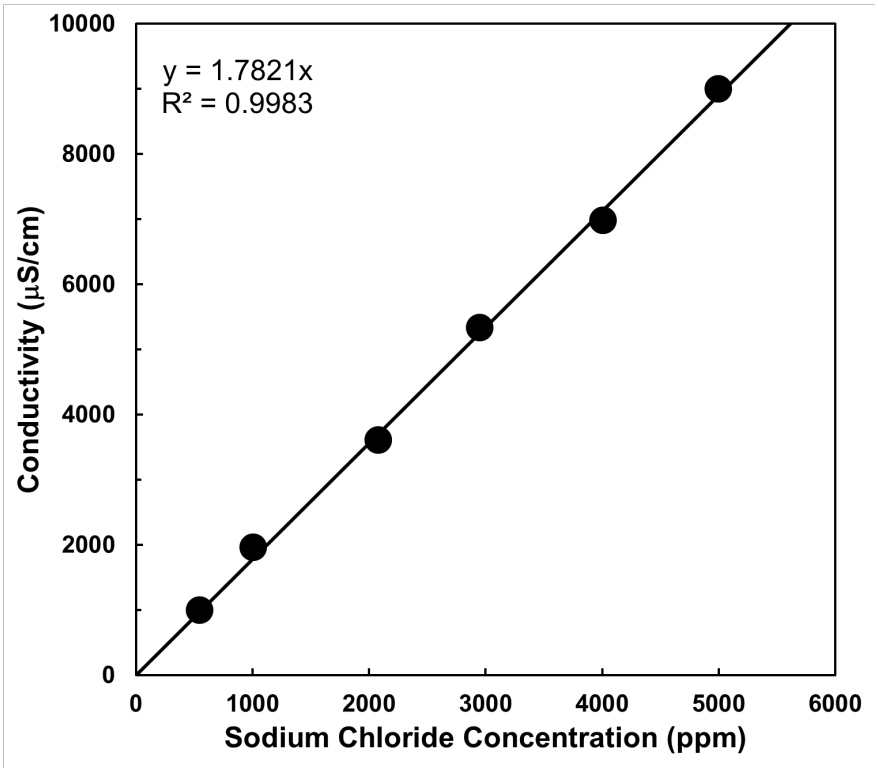

Figure 3. Relationship profile between conductivity (k = 1.0) and concentration of sodium chloride.

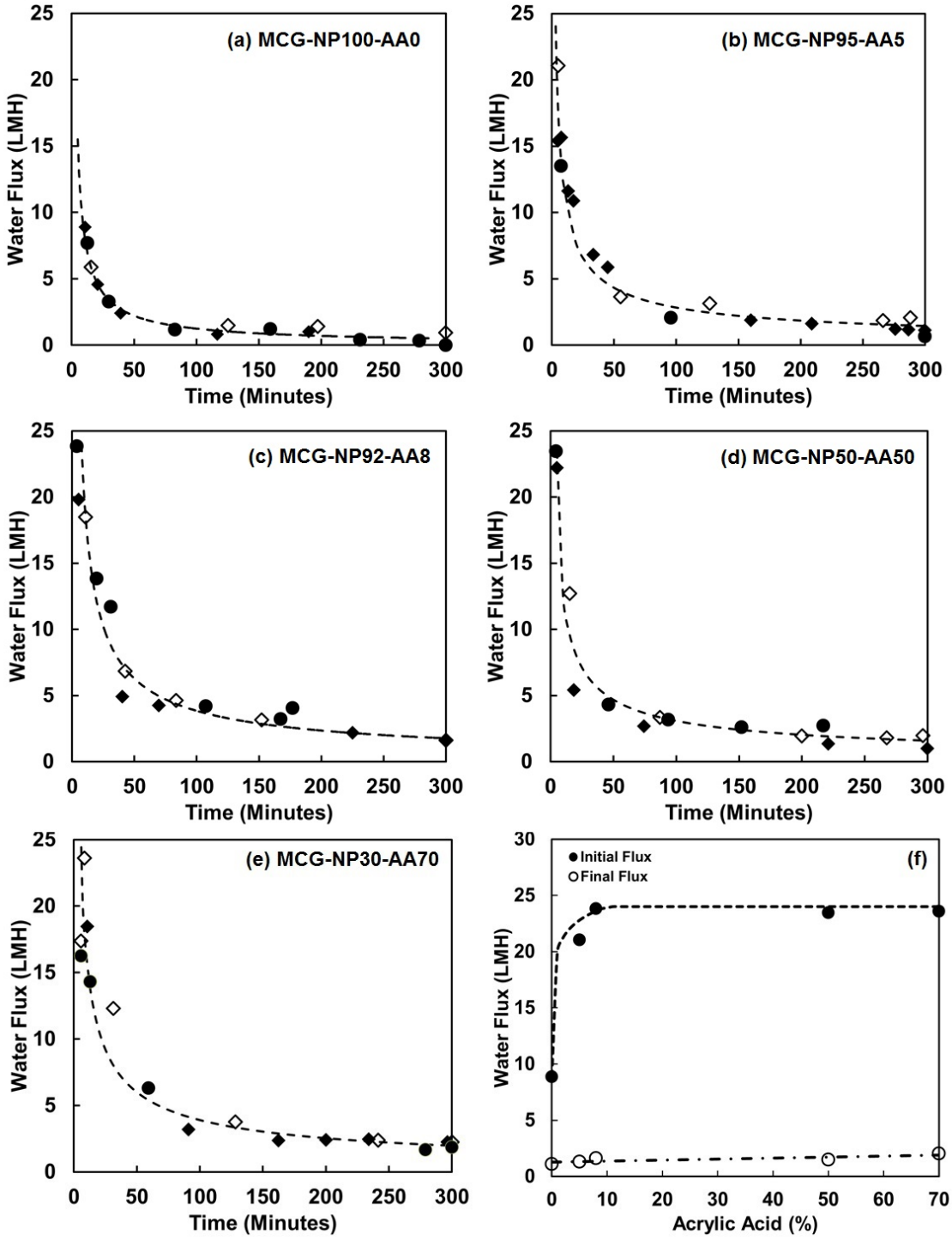

Figure 4. (a)-(e) Water flux for the co-polymer microgels with different acrylic acid contents over a five hour test period; and (f) effect of acrylic acid contents on the water flux.

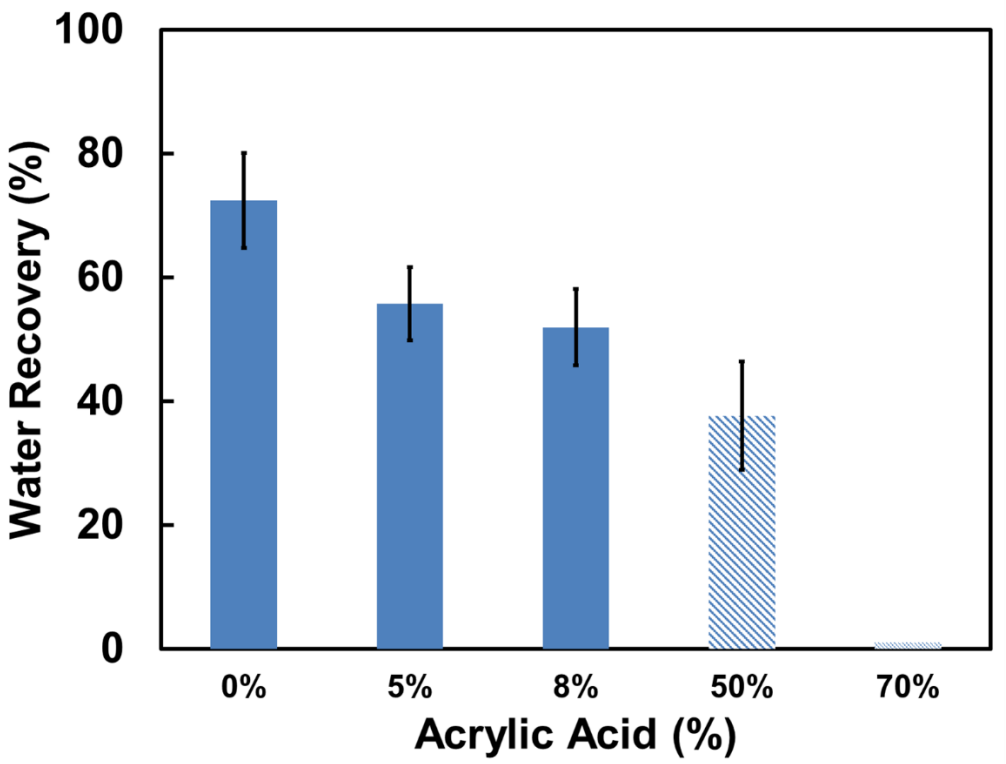

Figure 5. Water recovery ability of the co-polymer microgels with different acrylic acid contents (The pH of microgels with 50wt% AA is adjusted using hydrochloric acid).

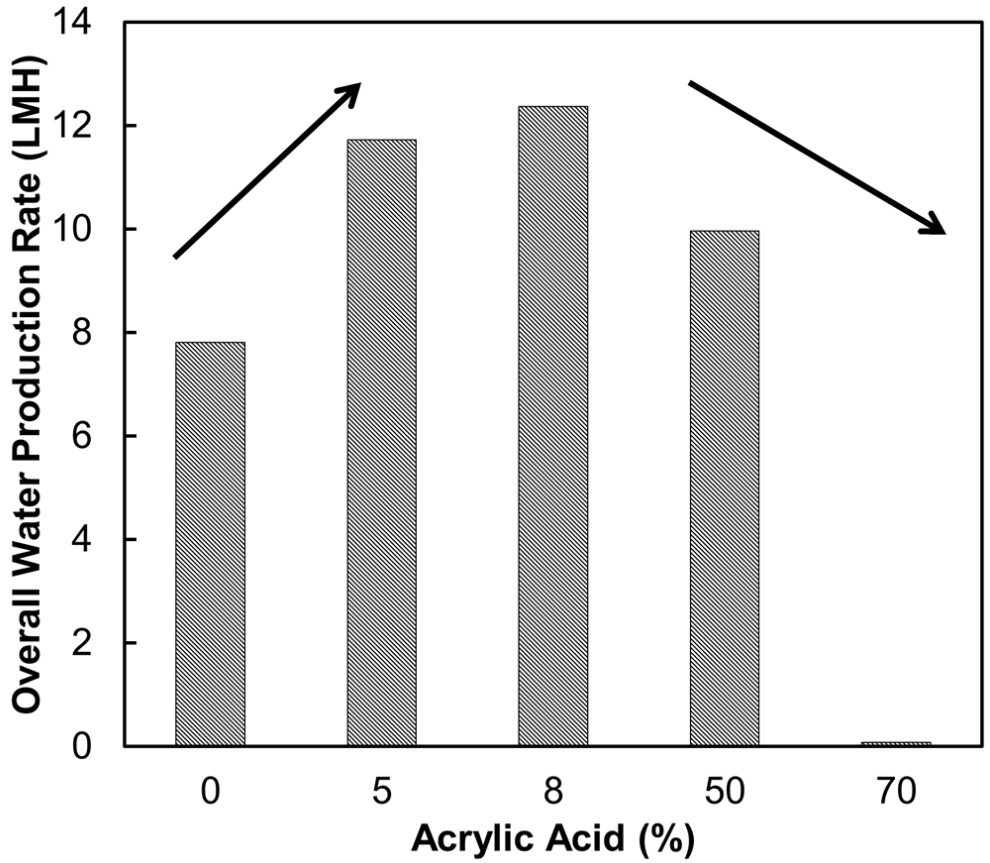

Figure 6. Effect of acrylic acid contents on the overall water production rates of the microgel-based FO process (Overall water production rate = water flux (LMH) x water recovery (%)).

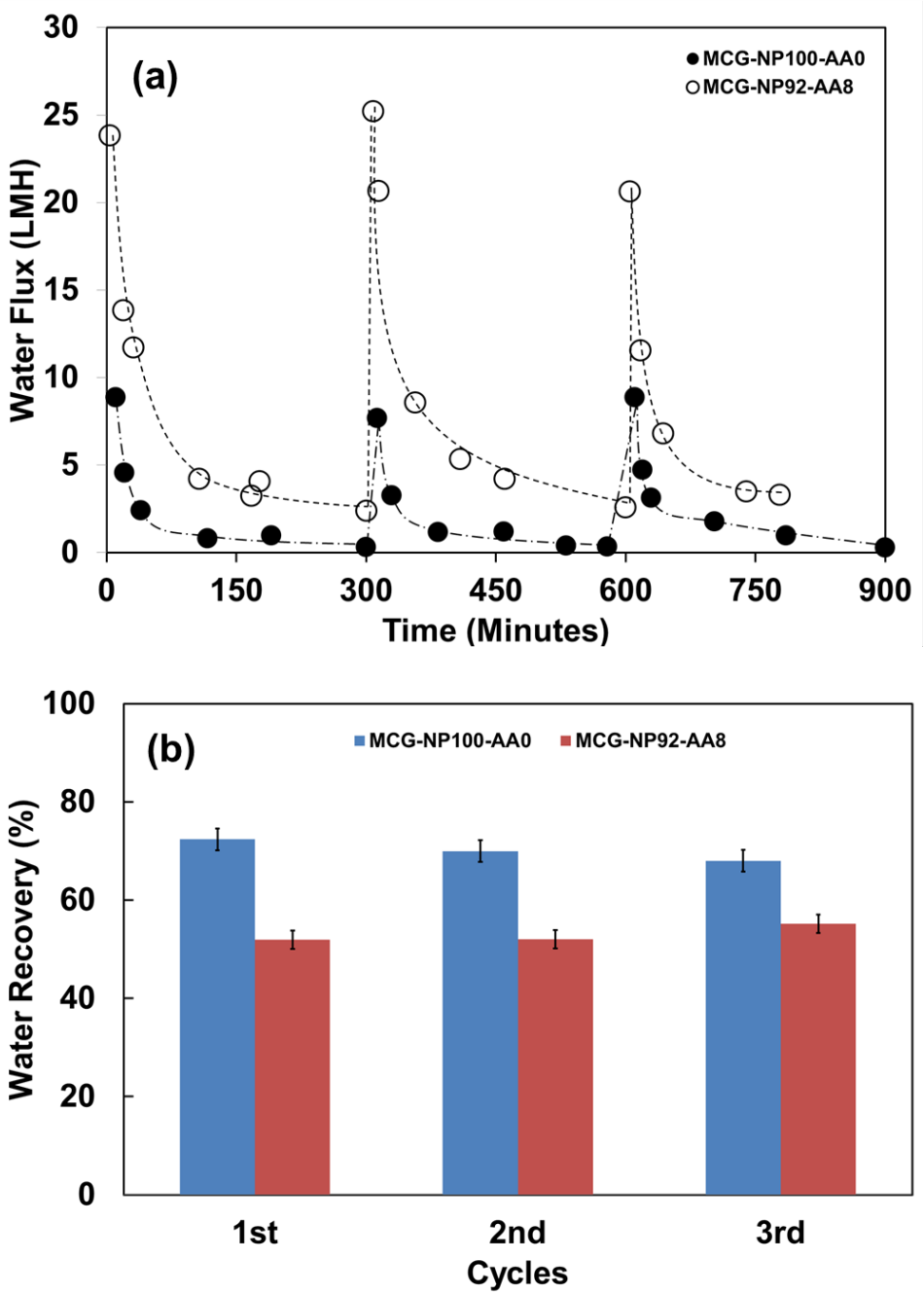

Figure 7. (a) Water flux profiles for MCG-NP100-AA0 and MCG-NP92-AA8 microgels for three consecutive cycles; and (b) water recovery for MCG-NP100-AA0 and MCG-NP92-AA8 microgels for three consecutive cycles.